Al-Qadisiyah Journal for Engineering Sciences 17 (2024) 267–272

Contents lists available at http://qu.edu.iq

Al-Qadisiyah Journal for Engineering Sciences

Journal homepage: https://qjes.qu.edu.iq

# Characteristic optimization of three-phase induction motors based on FEM

*Ahmed J. Ali* [1], *Abdullah K. Shanshal** [1], *Hiba Esam Aziz* [1], *and Essam Hussain* [2]

[1]*Electrical Power Technique Engineering. Engineering Technical College Mosul. Northern Technical University. Mosul. Iraq*
[2]*Principle Power Electronics Engineer Reseach, TAE Power Solutions, Birmingham, B37 7YG, UK*

ARTICLEINFO

*Article history:*
Received 05 March 2024
Received in revised form 26 May 2024
Accepted 01 June 2024

*Keywords:*
*Squirrel cage induction motor*
*Rotor bar dimensions*
*Air gap design*
*The magnetomotive force*
Magnetic flux density

ABSTRACT

Induction motors (IMs) with varying torque-speed characteristics are widely employed in various industrial applications. However, designing an efficient induction motor requires some of the main parameters of the motor (torque, speed, and efficacy) to beinvestigated and optimized. Furthermore, due to the significant influence of the rotor slot configurations on the electromagnetic torque-speed envelope, a design optimization procedure is required to optimize the induction motor's dynamic characteristics. In this paper, the impact of rotor slots' geometrical modifications on the behavior of 3-phase, four poles, 36 slots, and double-layer squirrel cage IM are presented and considered as examples of optimization. Moreover, the effect of the air gap dimensionand bore diameter of the stator and rotor parts are investigated. The predicted results demonstrate that the constructed geometry of the rotor slots has an observable effect on the performance of an (IM).



## 1. Introduction

Squirrel cage-type IM is considered one of the most powerful electric machines. This is due to the basic construction of rotor parts, robustness, and high efficiency [1]. However, it is critical to understand the required machine performance, such as its efficiency, torque-speed characteristics, current and voltage requirements, and the application for which it is being developed. The desired rotor resistance and inductance characteristics of the IMs as a function of slip frequency must be analyzed and matched with acceptable rotor bar geometry [2]. The skin effect is essential in the bar, especially in deep-bar designs which exploits to improve the starting performance of cylindrical cage-type machines. Consequently, during startup, it has a high AC resistance and a low inductance [3,4].

The rotor resistance and rotor leakage reactance are affected by the cross-sectional area of the rotor slot [5,6]. The rotor and stator material type is an important factor and should be considered while investigating IM starting performance taking into account the skin effect and leakage flux saturation with cast aluminium or copper rotors [7].

The geometries of squirrel cage induction motors (SCIMs) with different shapes of rotor bars such as rectangular, trapezoidal, T-inverse, and other geometrical shapes are considered as an important leading parameter and should be investigated precisely, taking into consideration the skin effect and saturation effect. [8]. The ratio of bar height to bar thickness is also an important factor and is recommended to be considered correctly in the geometry optimization of IMs, due to the direct effect of the starting torque and the starting current [9].

The effectiveness of rotor slot dimensions on the power factor, torque, and efficiency of the motor is investigated in [10]. A variation of rotor bar dimension and area has a direct effect on the rotor current and rotor flux linkage causing the variation in the magnitude of the electromagnetic torque generated in the rotor [11]. On the other hand, the shorter and wider slot openings play an effective role in producing better-locked rotor torque and a better force factor. While the use of deeper and broader slot dimensions will produce higher operating efficiency [12].

* *Corresponding author.*
E-mail address: a.shanshal@ntu.edu.iq (Abdullah Shanshal)

https://doi.org/10.30772/qjes.2024.147485.1153

**Nomenclature:**

| | | | |
|---|---|---|---|
| $l_g$ | Length of air gap | $l_g$ | The length of air-gap |
| $\mu_0$ | Air permeability ($4\pi e^{-7}$) | $\mu_0$ | An Air permeability which is a ($4\pi e$-7) |
| L | Stack length | $B_{av}$ | A specific magnetic loading |
| $Y_S$ | Slot pitch | $K_g$ | The Carters gap coefficient |
| $W_s$ | The width of the slot. | | |

Maxwell software is one of the recommended FEA software used in optimizing processes. The main design parameters of SCIM such as changing the rotor slot type, stator slot type, steel sheet, and rotor material, analyzing the output and predicting results to obtain the most efficient characteristics can be optimized by Maxwell [13]. The materials of conductor bars such as silicon, copper, and aluminium can be utilized through different finite element approaches to estimate the input and output power relationships to compute the resultant torque. Consequently, the result confirms that the starting current is significantly reduced when silicon copper is used to create a long-neck shape [14]. Using the parametric approximation approach IMs performance is altered by varying the rotor bar's structure, which has a direct influence on magnetic and electrical circuit models [15]. The investigation shows that the efficiency rises as the slot structure changes; with the decrease in rotor resistance, the rated torque falls. The size of the rotor slot structure has an important effect on the weight of the motor [16]. The genetic algorithms approach ae used to study the geometrical dimensions of the IM's stator and also, rotor bars parametrically [17]. The algorithm uses the survival of the fittest concept to identify improved approximations to achieve the goal, the GA will often involve the three basic genetic operations of selection, crossover, and mutation. The process of choosing individual possible solutions (individuals) based on their level of fitness results in a fresh set of approximations at the end of each generation [18]. The predicted results clearly show that the leakage inductance should be kept to a small value to improve the breakdown torque and to get a wide speed range. However, higher breakdown torque is produced by shorter and wider stator-slot shapes. In this paper, the investigation of induction motor geometry is presented. More specifically, the effect of the rotor bar variation with air gap is analyzed using multi-objective genetic algorithms in Ansys Maxwell software. Furthermore, to study the observation of the variations of the magnetic flux distribution in the airgap by changing the diameter of the airgap, as well as the effect of this change on the losses in the rotor and the overall efficiency of the induction motor.

### 1.1. Rotor design aspect

The slot design of the IM has a significant impact on its performance. For conventional motors deep slots are frequently used to improve start-up characteristics which results in a significant skin effect and increased rotor leakage resistance. Consequently, to reduce rotor leakage resistance, constructions with different slot geometries are employed, which will then increase the starting torque and power factor (PF) [19].

On the other hand, an interaction between the basic magnetomotive force (MMF) and harmonics of magnetic conductivity depends on the width of the slot opening. Therefore, utilizing a semi-enclosed slot reduces copper loss and the motor's harmonic current, as well as the harmonics that the slot generates [20,21] Furthermore, it is necessary for the structure of the slot to be wide at the top and thin at the bottom to achieve a parallel tooth structure for superior quality so that high-frequency harmonics can be efficiently eliminated [9]. The effect of the rotor slot can be summarized as follows where the $h_{r0}$, $h_{r1}$, $h_{r2}$, $b_{r0}$, $b_{r1}$, and $b_{r2}$ are the dimensions of the rotor slot shown in Table 1.

1. The opening bar's width, $b_{r0}$: Both noise and magnetizing current are decreased when the slot opening is narrow. But it raises the reactance of zigzag leakage. It may have an impact on the leakage inductance and air-gap permeance of the motor. On the other hand, the smallest feasible hole is preferable [22,23].
2. The width of slot arms $b_{r1}$ & $b_{r2}$: The rotor slot must be constructed with a narrow bottom half and a broad upper segment, according to the design idea. To avoid the large range of optimizing parameters and the high effort, the two variables ($b_{r1}$ and $b_{r2}$) are optimized individually in a variety of ranges by unique rules related to the mechanical design [22,23].
3. The height of the slot head is ($h_{r0}$): It is better to be a small value, which can be considered equal to the slot opening effect on the design [23].
4. Height of slot $h_{r2}$: The rotor slot's current density changes as a result of the slot's area changing as the value changes. The efficiency of the motor and rotor copper loss is impacted by variations in current density (J) [24]. The rotor leakage reactance increases and the rotor resistance decreases with increasing rotor slot area [25,26]. A relative equilibrium in the efficiency value may be attained with the appropriate selection of the $h_{r2}$ value.

**Table 1.** Rotor Dimensions of the proposed IM

| Symbol | Definitions of symbol | Value (mm) |
|---|---|---|
| $h_{r1}$ | The height of the slot head | 0.6 |
| $h_{r2}$ | Height of slot | 12 |
| $b_{r0}$ | The width of slot opening | 2 |
| $b_{r1}$ | width of slot shoulder | 4 |
| $b_{r2}$ | The width of the slot arm | 2 |

### 1.2. Flux line transfers

The magnetomotive force (MMF) in the air gap of the IM is initially affected based on the opening width of the bar, in other words, by the type of the bar itself, whether it is closed, open, or semi-open [25,26]. Moreover, the transmission of the magnetic flux lines from the stator to the rotor through the air gap is affected by several factors, including the material the motor is made of, as well as the type of bar. The following cases show the difference:

*Case 1:* As shown in Figure (1) the smooth iron surface on both sides of the air gap; the flux line's transition is straight and uniform. The reluctance of the air gap can be calculated as [27]:

$$S_g = \frac{l_g}{\mu_0 * A} \quad (1)$$

$$S_g \frac{l_g}{\mu_0 * L * Y_S} \quad (2)$$

Case 2: Open rotor bar Figure (2) shows the magnetic flux lines in the case of an open bar with concentration in the tooth width. Consequently, the effectiveness of air gap flux is decreased, and the reluctance of air-gap is increased and could be calculated [27]:

$$S_g = \frac{l_g}{\mu_0 * L * (Y_S - W_S)} \quad (3)$$

The MMF in air gap with open and semi-closed slots is calculated as:

$$MMF = \frac{B_{av}}{\mu_0} * K_g * l_g \quad (4)$$

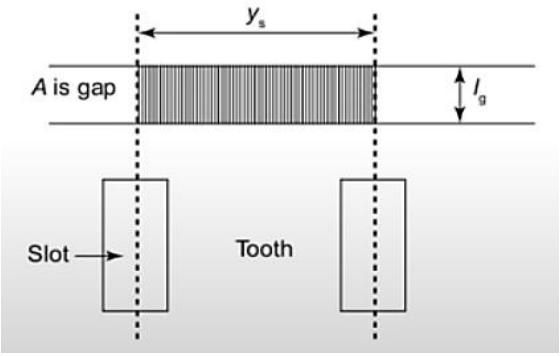


**Figure 1.** Flux Line Form in Air Gap with Closed Rotor Bar

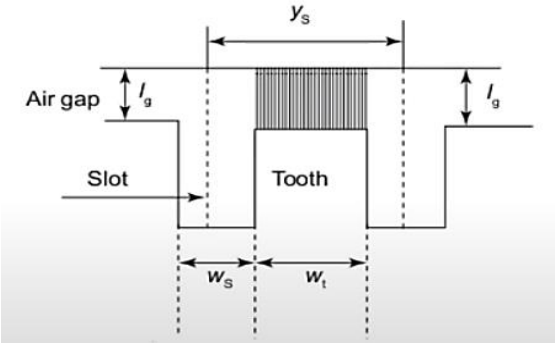


**Figure 2.** Flux Line form at the Type of Opening Slot [27]

### 1.3 Design optimization

The optimization for a proposed three-phase induction motor involves four steps as illustrated in Figure (3), it starts with the implementation of a basic model of a motor with fixed parameters such as the number of pole pairs, stator number of slots, stator, and- rotor slot dimensions and rotor number of slots. After that the initial design is simulated and analytical model behaviour is examined by torque waveform, output power, efficiency, as well as power factor [28]. Furthermore, the initial design is verified by finite Element Analysis for verification. Moreover, the multi-objective optimization methodology is performed using a multi-objective genetic Algorithm (MOGA) method taking into account the effect of changing the rotor bar dimensions to study the machine's performance and enhance efficiency [29].

## 2. Simulation results and discussion

Optimization methodologies for different parts of the induction motor are carried out to improve performance and increase efficiency. However, the rotor bar resistance is inversely proportional to cross-sectional and, conductivity. The rotor resistance increases with the decreasing of the cross-section area since the SCIM at the starting affects the skin so these influences will change the performance of the motor. Furthermore, the length of the air gap between the stator and rotor influences motor performance in terms of overload capacity, magnetizing current, thermal considerations, and vibration & noise [30]. An extremely narrow air gap leads to increased harmonics and losses. While a wide air gap affects efficiency and power factor. Consequently, for the proposed optimized model air-gap dimension is reduced during the optimization from (0.5 mm to 0.4 mm), which leads to an increase in the power factor from (0.75 to 0.83) P.U [31,32], this can be predicted as shown in Figure (4).

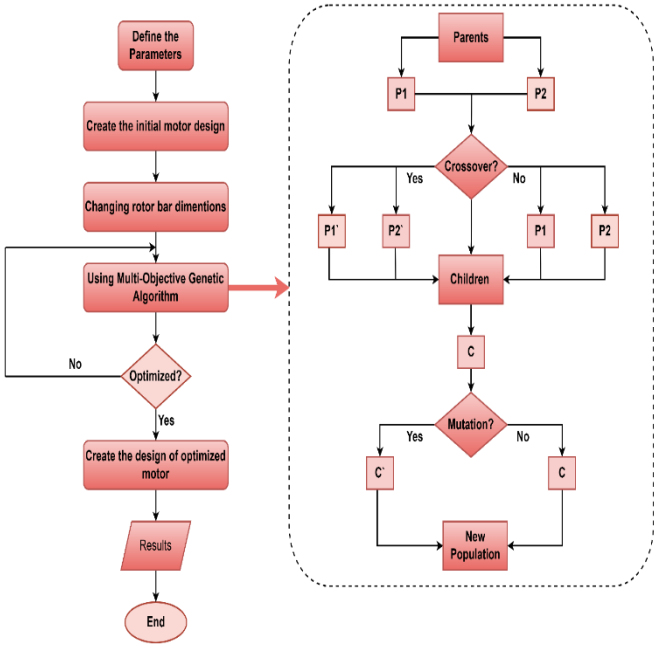


**Figure 3.** Algorithm Flowchart with the Proposed Methodology [30]

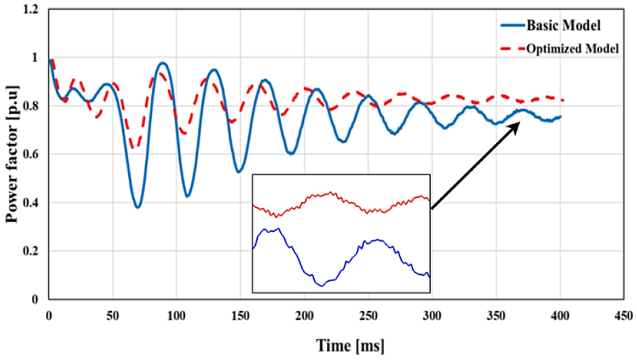


**Figure 4.** Power Factor for Basic and Optimized Motor

The flux linkage, absorbed from the stator and crossing to the rotor part through the air gap has a considerable influence on the cross-sectional area of a rotor bar [33,34]. However, there will be certain flux lines that do not flow between the stator and rotor, causing a flux leakage that may be seen at the slots and air gap (zigzag leakage), as shown in Figure (5). It can be noticed that compared to the basic model the leakage flux across the air gap for the optimized model is reduced, and this means that it

moved to the rotor better in the improved model. Moreover, a high current density produces a large torque, which has a positive effect on the starting performance, Figures (6-&7) illustrate the linkage flux and current density distribution lines and waveforms in the rotor bar. Consequently, the predicted waveform shows an increase in flux line through the rotor bar by (7.78%) for the optimized proposed model [35].

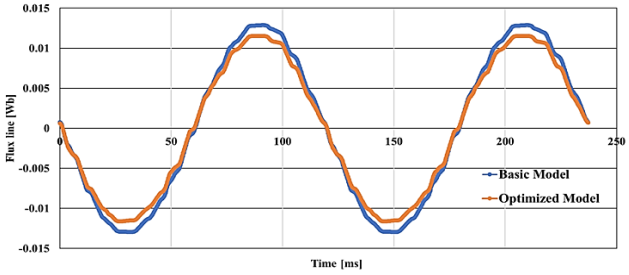


**Figure 5.** Flux Line Pass-Through Air Gap

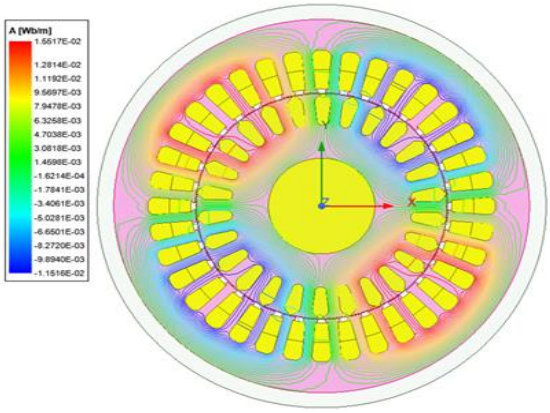


**Figure 6.** Flux Line in Optimized Proposed Model

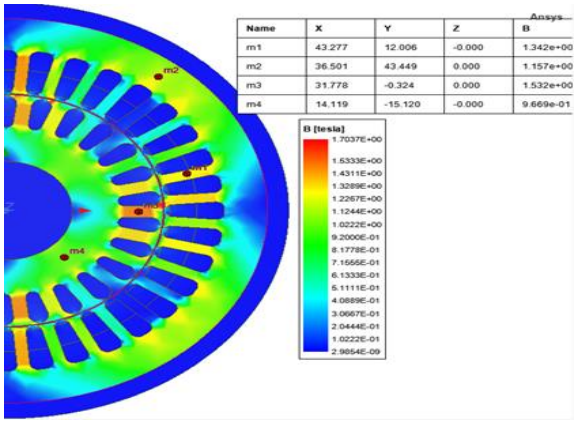


**Figure 7.** Magnetic Flux Density in Optimize Model

The optimized value of slot opening width (1.45 mm) as well as the estimated value of the airgap length (0.4 mm), have an effective role in increasing and capturing the maximum value of the linkage flux through which a maximum value of the magnetic and electric loading characteristics can be achieved [36], Figures (8 & 9) depict the MMF waveforms in the air gap region as well as the estimated harmonics.

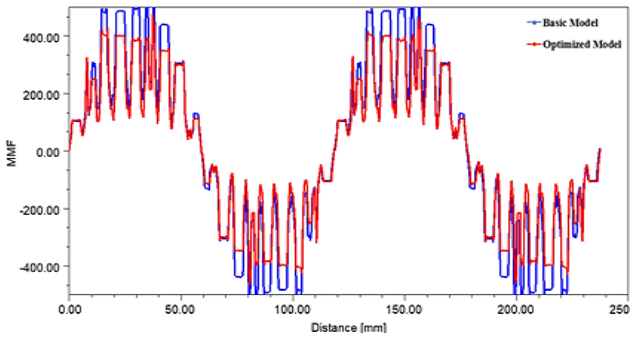


**Figure 8.** MMF in Air Gap for Basic and Optimized Model

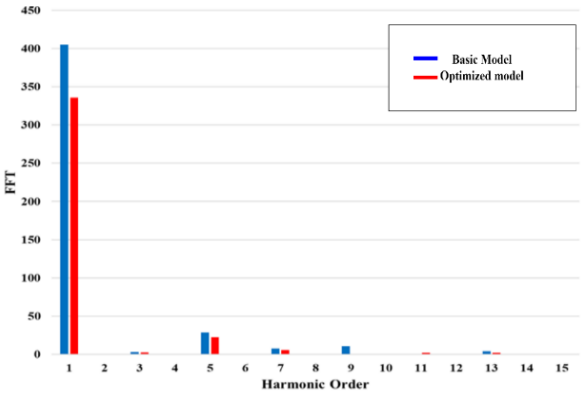


**Figure 9.** Harmonic of Air Gap for Basic and Optimized Model

## 3. Conclusion

Optimization methodologies for different parts of the induction motor are carried out to improve performance, to increase efficiency, and to be a good contender for different industries, domestic, andelectric vehicle applications. This paper focuses on changing the dimensions of the rotor bar and studying the associated effect that may occur in the model performance.

The proposed geometry of the SCIM model is simulated and modeled using the Maxwell Ansys software based on two steps: firstly, by utilizing the RMXprt property and secondly, by implementing the mechanical laws of design through the program's parametric drawing feature.

Moreover, the optimization processes are executed based on the genetic algorithm strategy, including multi-objective and random genetic algorithms. The detected results showed that changing the shape of the bar in addition to the size of the air gap will increase the work efficiency and the power factor to 10.67% by reducing the leakage flux occurring in the gap during transmission. On the other hand, reducing harmonics and improving the amount of current induced through the rotor bar by 38%, will reduce copper losses, which in turn also contributes to increased motor efficiency by 6.67%.

## Acknowledgments

The authors would like to express particular thanks to everyone in the Department of Electrical Power Engineering Techniques/ Engineering

Technical College, Mosul and TAE. Technologies Solution Company, UK who supported and encouraged us throughout the whole research process.

## REFERENCES


[1] E. Engineering, "Modeling of Rotor Bars in Induction Motors with Special Focus on Starting Performance Saeed Rahimi," Science (1979), 2006. https://doi.org/ 10.1109/ISIE51358.2023.10227958

[2] A. I. Çanakoğlu, A. G. Yetgin, H. Temurtaş, and M. Turan, "Induction motor parameter estimation using metaheuristic methods," Turkish Journal of Electrical Engineering and Computer Sciences, vol. 22, no. 5, pp. 1177–1192, 2014, https://doi.org/10.3906/elk-1211-171.

[3] A. Boglietti et al., "Analysis and Modeling of Rotor Slot Enclosure Effects in High-Speed Induction Motors," pp. 154–161, 2011. https://doi.org/10.1109/ECCE.2011.6063763

[4] J. Kappatou, K. Gyftakis, and A. Safacas, "FEM study of the rotor slot design influences on the induction machine characteristics," Studies in Applied Electromagnetics and Mechanics, vol. 30, no. June, pp. 247–252, 2008, https://doi.org/10.3233/978-1-58603-895-3-247.

[5] A. Barbour, W. T. Thomson, and S. Member, "finite element study of rotor slot designs with respect to current monitoring for detecting static airgap eccentricity in squirrel - cage induction motors," pp. 112–119, 1997. https://doi.org/ 10.1109/IAS.1997.643016.

[6] D. Hong, J. Choi, D. Kim, Y. Chun, B. Woo, and D. Koo, "Development of a High Speed Induction Motor for Spindle Systems," vol. 49, no. 7, pp. 4088–4091, 2013. https://doi.org/ 10.1109/TMAG.2013.2241033.

[7] "Electric Machines & Power Systems Performance Comparison of Optimally Designed Induction Motors with Aluminum and Copper Squirrel-Cages," no. November 2014, pp. 37–41, 2010, https://doi.org/10.1080/073135600449062.

[8] J. A. Redinz, "Concerning the Influence of the Rotor Bar Geometry on the Induction Motor Performances," Eur J Phys, vol. 36, no. 5, pp. 647–650, 2015, https://doi.org/10.1088/0143-0807/36/5/055008.

[9] S. Williamson, "Calculation of the bar resistance and leakage reactance of cage rotors with closed slots," IEE Proceedings B: Electric Power Applications, vol. 132, no. 3, pp. 125–132, 1985, https://doi.org/10.1049/ip-b.1985.0018.

[10] P. Pao-La-Or, S. Peaiyoung, T. Kulworawanichpong, and S. Sujitjorn, "Effects of the geometry of the rotor slots on the mechanical vibration of three-phase induction motors," in SMO'07 Proceedings of the 7th WSEAS International Conference on Simulation, Modelling and Optimization, 2007, pp. 435–439. https://doi.org/10.1049/cp:19971106.

[11] C. Paper and J. Kappatou, "FEM Study of the Rotor Slot Design Influences on the Induction Machine Characteristics FEM study of the rotor slot design influences ON," no. June, 2021, https://doi.org/10.3233/978-1-58603-895-3-247.

[12] A. G. Yetgin and B. Durmuş, "Analysis of the effect of rotor slot type on torque ripple in induction motors by finite element method," El-Cezeri Journal of Science and Engineering, vol. 7, no. 2, pp. 536–542, 2020, https://doi.org/ 10.31202/ecjse.664132.

[13] M. Tumbek, Y. Oner, and S. Kesler, "Optimal Design of Induction Motor with Multi-Parameter by FEM Method Optimal Design of Induction Motor with Multi-Parameter by FEM Method," no. November, pp. 2–6, 2015, https://doi.org/10.1109/ELECO.2015.7394483.

[14] G. Lee, S. Min, and J. P. Hong, "Optimal shape design of rotor slot in squirrel-cage induction motor considering torque characteristics," IEEE Trans Magn, vol. 49, no. 5, pp. 2197–2200, 2013, https://doi.org/10.1109/TMAG.2013.2239626.

[15] A. Gokhan Yetgin and M. Turan, "Effects of Rotor Slot Area on Squirrel Cage Induction Motor Performance," IJISET-International Journal of Innovative Science, Engineering & Technology, vol. 3, no. 11, pp. 105–109, 2016, [Online]. Available: www.ijiset.com

[16] J. K. Kammoun, N. Ben Hadj, M. Ghariani, and R. Neji, "Torque ripple and harmonic density current study in induction motor: Two rotor slot shapes," International Review on Modelling and Simulations, vol. 8, no. 2, pp. 197–204, 2015, https://doi.org/10.15866/iremos.v8i2.5568.

[17] Y. S. Kim, "Effects of rotor bar shape for squirrel cage induction motor in transient state using moving band technique," IEEE Transactions on Applied Superconductivity, vol. 24, no. 3, pp. 1–4, 2014, https://doi.org/10.1109/TASC.2013.2292072.

[18] W. Purwanto, T. Sugiarto, H. Maksum, M. Martias, M. Nasir, and A. Baharudin, "Optimal design of rotor slot geometry to reduce rotor leakage reactance and increase starting performance for high-speed spindle motors," Advances in Electrical and Electronic Engineering, vol. 17, no. 2, pp. 96–105, 2019, https://doi.org/10.15598/aeee.v17i2.3170.

[19] V. Aguiar, R. Pontes, and T. Fernadoes Neto, "Parameters Estimation of Squirrel Cage Induction Motors with Closed Rotor Slots," no. March, p. 2, 2016. https://doi.org/10.14381/bajece.716742

[20] B. M. Saied and A. J. Ali, "Determination of deep bar cage rotor induction machine parameters based on finite element approach," 2012 1st National Conference for Engineering Sciences, FNCES 2012, no. November 2018, 2012, https://doi.org/10.1109/NCES.2012.6740481.

[21] A. J. Ellison, "Electric Machinery and Control," Electronics and Power, vol. 11, no. 4, p. 144, 1965, https://doi.org/10.1049/ep.1965.0114.

[22] Y. Shen, C. Zhu, and X. Wang, "Slot Optimization Design of Induction Motor for Electric Vehicle," IOP Conf. Ser. Mater. Sci. Eng., vol. 301, no. 1, 2018, https://doi.org/10.1088/1757-899X/301/1/012081.

[23] A. Boglietti, S. Member, A. Cavagnino, and M. Lazzari, "Geometrical Approach to Induction Motor Design," no. 1, pp. 149–156, 2007. https://doi.org 10.1109/IEMDC.2019.8785233

[24] M. REZAIEE NAKHAIE and R. roshanfekr, "Effects of Geometric Dimension Variations on Efficiency of 3-phase Squirrel Cage Induction Motors Considering Economic Evaluation," Balk. J. Electr. Comput. Eng., no. November, 2022, https://doi.org/10.17694/bajece.732721.

[25] L. Alberti, N. Bianchi, S. Member, and S. Bolognani, "Variable-Speed Induction Machine Performance Computed Using Finite-Element," vol. 47, no. 2, pp. 789–797, 2011. https://doi.org/10.1109/TIA.2010.2103914

[26] A. Shanshal, K. Hoang, and K. Atallah, "High-Performance Ferrite Permanent Magnet Brushless Machines," IEEE Trans Magn, vol. 55, no. 7, 2019, https://doi.org/10.1109/TMAG.2019.2900561.

[27] A. K. Sawhney, Dhanpat Rai & Co., A course in electrical machine design. pp. 1–600, 2017. https://doi.org/10.14684/bajece.738741.

[28] A. K. Shanshal, A. J. Ali, and A. H. Al-Rifaie, "Study the dynamic performance of PM machines for different rotor topologies," International Journal of Power Electronics and Drive Systems, vol. 13, no. 4, pp. 2062–2070, 2022, https://doi.org/10.11591/ijpeds.v13.i4.pp2062-2070.

[29] H. Friends, "GA based optimal design of three-phase squirrel cage induction motor for enhancing performance," no. Iv, pp. 1–12, 2011. https://doi.org/10.12686/bajeol.736771.

[30] M. Khashan, D. Khudhur, and H. Balla, "Comparison between the two methods of optimization: Genetic algorithm (GA) and ant colony algorithm (ACO) for the propulsion system of UAV," Al-Qadisiyah J. Eng. Sci., vol. 16, no. 2, pp. 92–95, 2023, https://doi.org/10.30772/qjes.v16i2.861.

[31] H. E.Aziz, A. K. Shanshal, and A. J. Ali, "Optimization of Induction Motor Rotor Bar Geometry Based on Genetic Algorithm," In 2023 International Conference on Engineering, Science and Advanced Technology (ICESAT), pp. 127-132. IEEE, 2023. https://doi.org/10.1109/ICESAT58213.2023.10347297.

[32] M. Al-Ibraheemi, M., Anayi, F., Wahhab Neamah, M., Hassan, Z. (2023). 'Parameters estimation of non-saturated permanent magnet synchronous machines by aid of statistical analysis', *Al-Qadisiyah Journal for Engineering Sciences*, 16(2), pp. 127-132. doi: 10.30772/qjes.v16i2.877

[33] P. Basil and M. Saied, "Determination of Deep Bar Cage Rotor Induction Machine Parameters Based on Finite Element Approach," no. May 2020, 2012. https://doi.org/10.1109/NCES.2012.6740481.

[34] J. A. Malagoli, J. R. Camacho, and M. V. F. da Luz, "Optimal electromagnetic torque of the induction motor generated automatically with Gmsh/GetDP software," Int. Trans. Electr. Energy Syst., vol. 31, no. 3, pp.

1–20, 2021, https://doi.org/10.1002/2050-7038.12773.

[35] R. K. Sakran and A. P. D. K. M. Ali, "Speed Control of Dtc-Svm for Induction Motor Drive Using Self-Tuning Fuzzy Pi Controller Ann Anfis," Al-Qadisiyah J. Eng. Sci., vol. 11, no. 3, pp. 293–308, 2019, https://doi.org/10.30772/qjes.v11i3.562.

[36] S. Ratheesh and J. Vins, "Control of self-excited induction generator based wind turbine using current and voltage control approaches," Al-Qadisiyah J. Eng. Sci., vol. 16, no. 3, pp. 209–217, 2023, https://doi.org/10.30772/qjes.2023.143509.1033.